

## Supporting Information

### **Insight into the mechanism of the solvolysis of propylene oxide over titanium silicalite-1: A theoretical study**

Qiaoyun Qin,<sup>a,b</sup> Hongxia Liu,<sup>c</sup> Yanke Guo,<sup>a,b</sup> Baohe Wang,<sup>a,b</sup> Jing Zhu,<sup>a,b,\*</sup> Jing Ma<sup>a,b,\*</sup>

<sup>a</sup> *Collaborative Innovation Center of Chemical Science and Engineering, Tianjin University, Tianjin 300072, China*

<sup>b</sup> *Key Laboratory for Green Chemical Technology of Ministry of Education, R&D Center for Petrochemical Technology, Tianjin University, Tianjin 300072, China*

<sup>c</sup> *School of Chemistry and Chemical Engineering, Wuhan Textile University, Wuhan, 430200, China*

---

\* Corresponding author at: No. 90 Weijin Road, Nankai District, Tianjin 300072, China. Tel.: + 86 22 27406959. Fax: +86 22 27406591 E-mail address: [majing0027@tju.edu.cn](mailto:majing0027@tju.edu.cn) (Jing Ma), [cj\\_zhu1975@tju.edu.cn](mailto:cj_zhu1975@tju.edu.cn) (Jing Zhu)

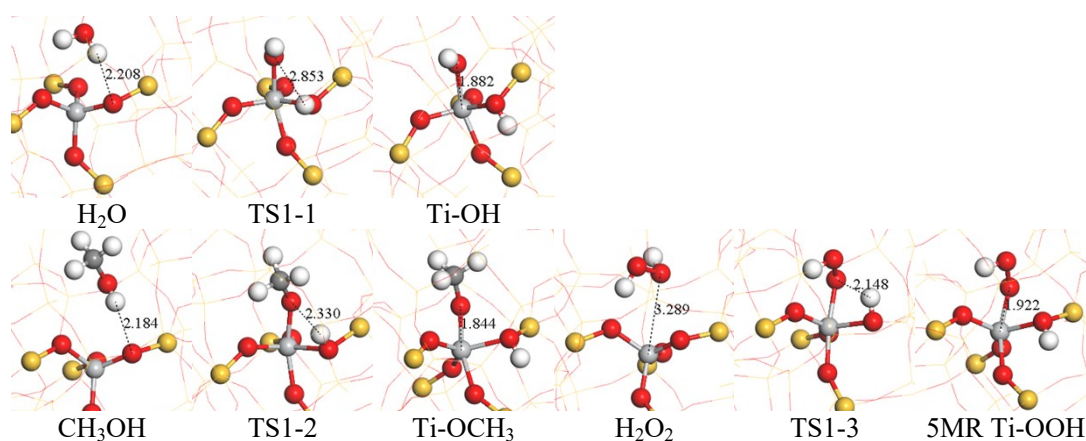
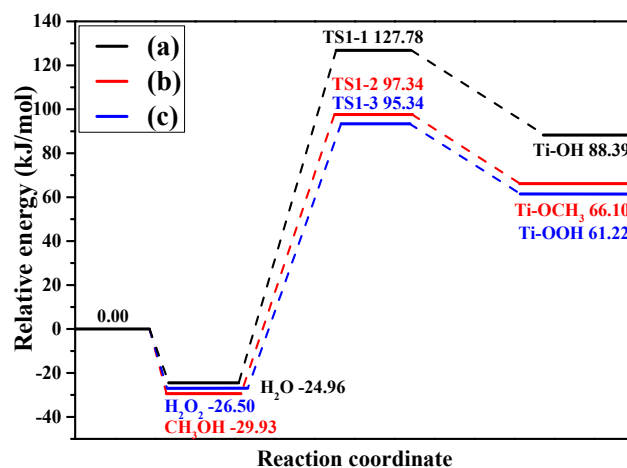


**Fig. S1** Potential energy profiles for formations of ring-opening active substances (a) Ti-OH, (b) Ti-CH<sub>3</sub> and (c) 5MR Ti-OOH at 313 K together with together with the structures of reactant, transition state and product at tetrahedral Ti site. The energy unit is in kJ/mol, and bond length is in Å. (Ti = light grey, C = grey, O = red, Si = yellow, H = white).

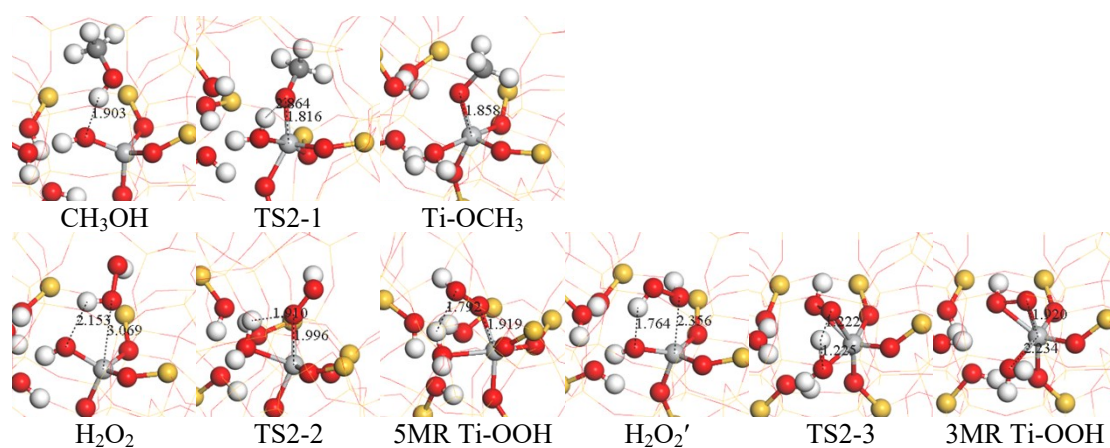
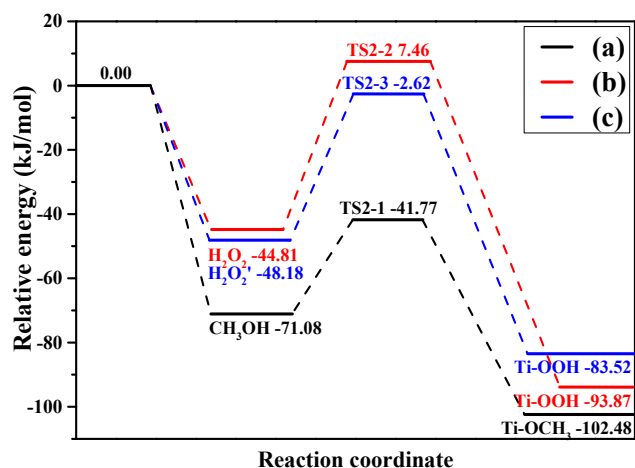


**Fig. S2** Potential energy profiles for formation of ring-opening active substances (a) Ti-OCH<sub>3</sub>, (b) 5MR Ti-OOH and (c) 3MR Ti-OOH at 313 K together with together with the structures of reactant, transition state and product at Ti/defect site. The energy unit is in kJ/mol, and bond length is in Å. (Ti = light grey, C = grey, O = red, Si = yellow, H = white).

Tetrahedral Ti site

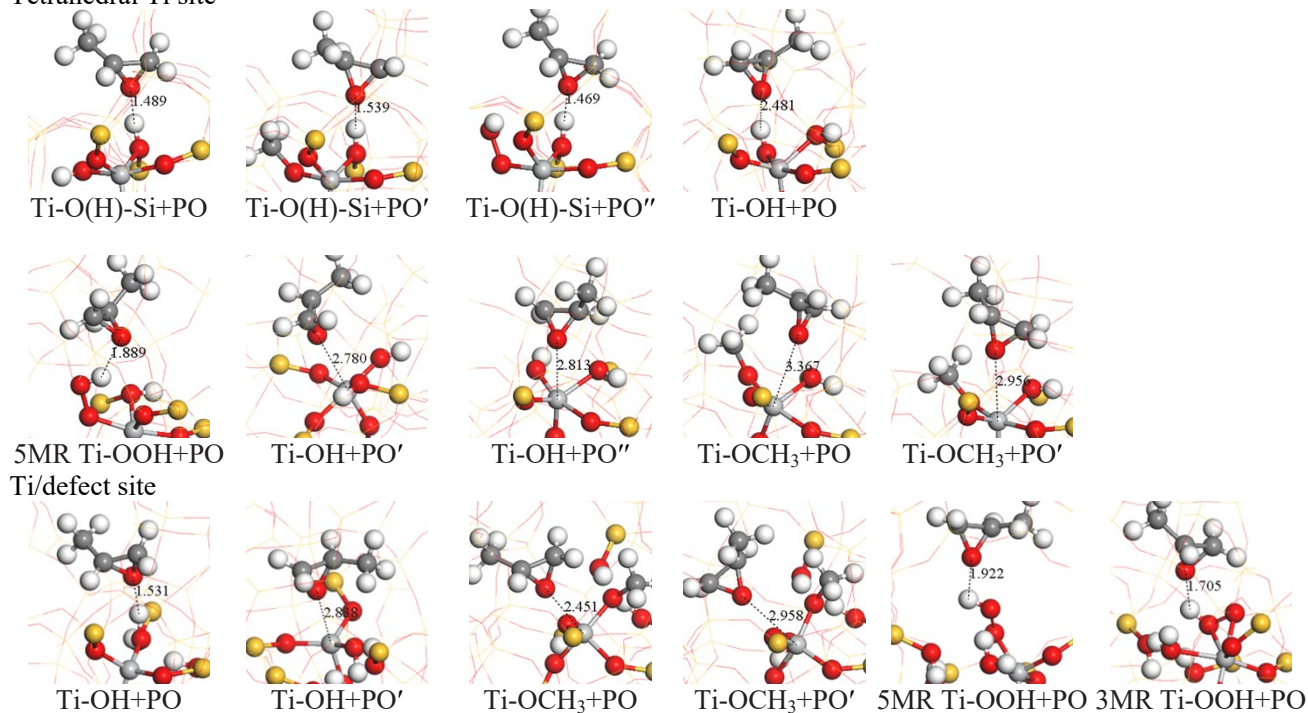


**Fig. S3** The stable adsorption configurations of PO over Ti-O(H)-Si, Ti-OH, Ti-OCH<sub>3</sub>, 5MR Ti-OOH and 3MR Ti-OOH together with the corresponding adsorption free energies at 313 K. The energy unit is in kJ/mol, and bond length is in Å. (Ti = light grey, C = grey, O = red, Si = yellow, H = white).

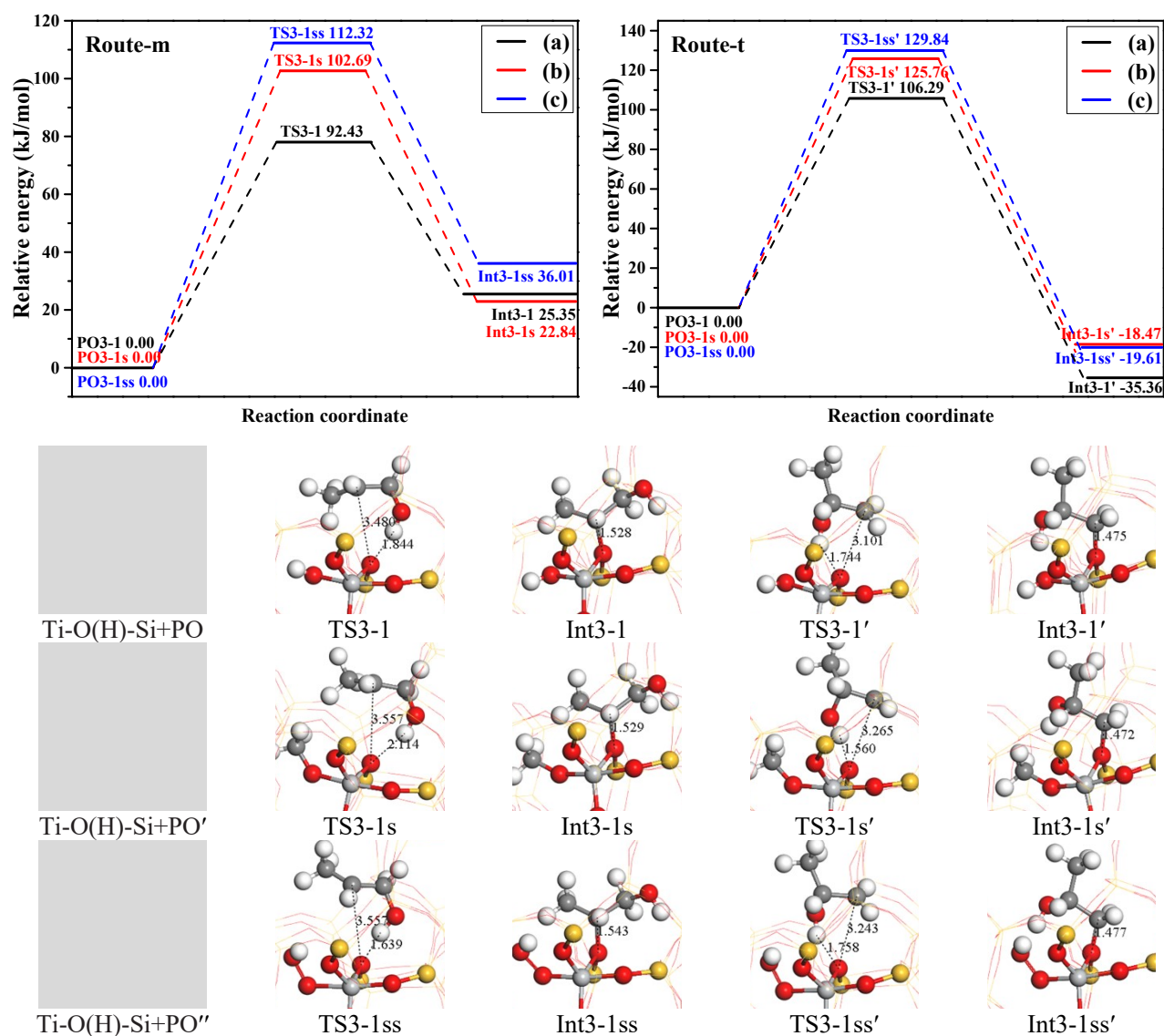


**Fig. S4** Potential energy profiles for the Brønsted acid reactions mode of ring-opening of PO with Ti-O(H)-Si adjacent to (a) -OH, (b) -OCH<sub>3</sub> and (c) -OOH groups at 313 K together with together with the structures of reactant, transition state and product at tetrahedral Ti site. The energy unit is in kJ/mol, and bond length is in Å. (Ti = light grey, C = grey, O = red, Si = yellow, H = white).

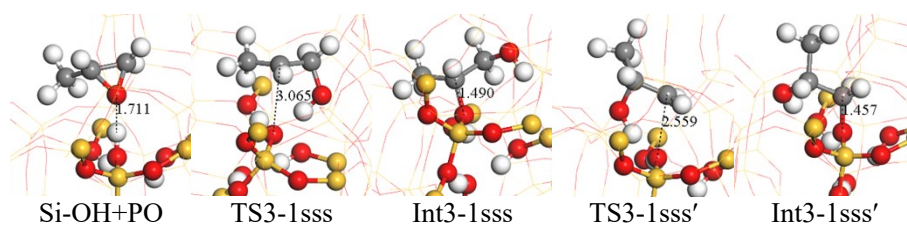
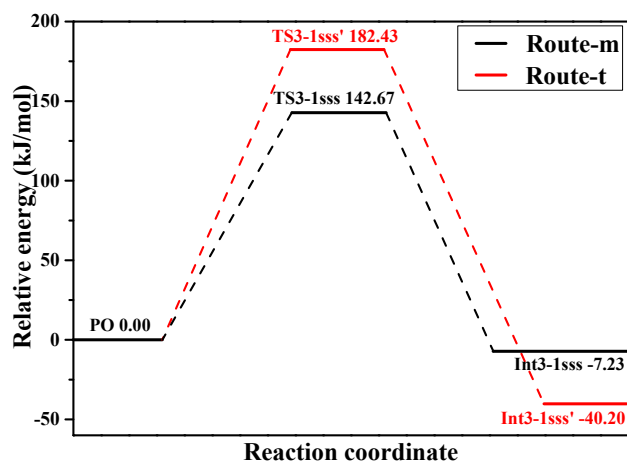


**Fig. S5** Potential energy profiles for the Brønsted acid reactions mode of ring-opening of PO with Si-OH at 313 K together with together with the structures of reactant, transition state and product. The energy unit is in kJ/mol, and bond length is in Å. (C = grey, O = red, Si = yellow, H = white).

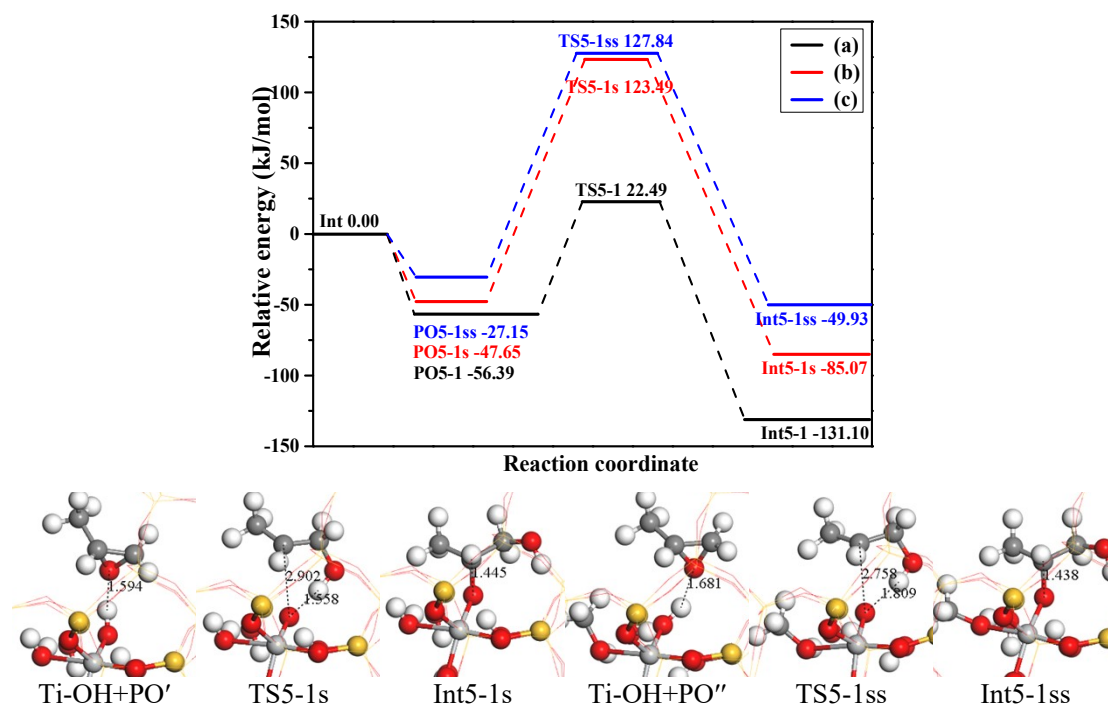


**Fig. S6** Potential energy profiles for the Brønsted acid reactions mode of ring-opening of PO with Ti-OH when co-adsorption with a (b) H<sub>2</sub>O or (c) CH<sub>3</sub>OH at 313 K together with together with the structures of reactant, transition state and product at Ti/defect site. The energy unit is in kJ/mol, and bond length is in Å. (Ti = light grey, C = grey, O = red, Si = yellow, H = white).



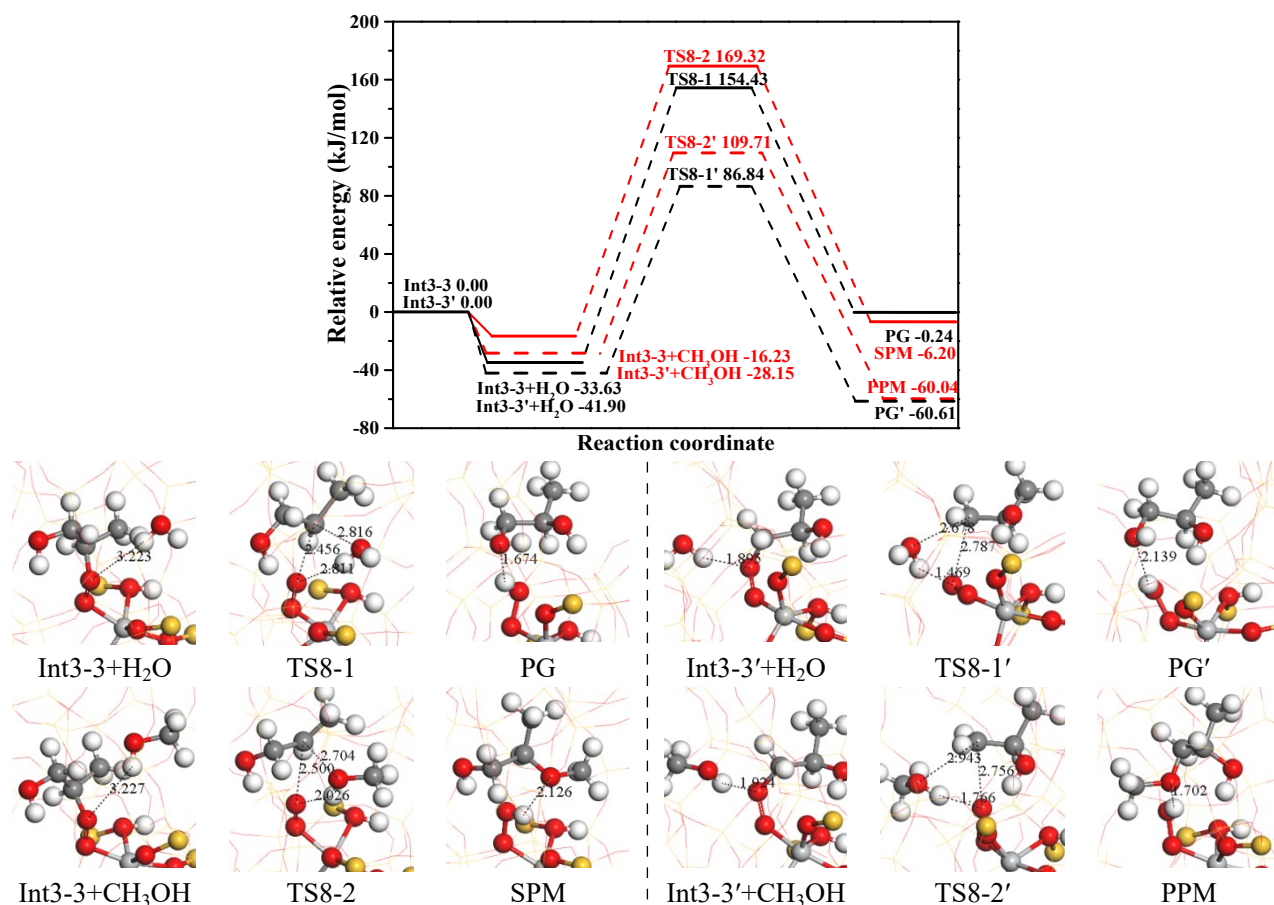


**Fig. S7** Potential energy profiles of PG, SPM and PPM formation via 5MR Ti-OOH at 313 K, together with the structures of reactant, transition state and product at tetrahedral Ti site. The energy unit is in kJ/mol, and bond length is in Å. (Ti = light grey, C = grey, O = red, Si = yellow, H = white).



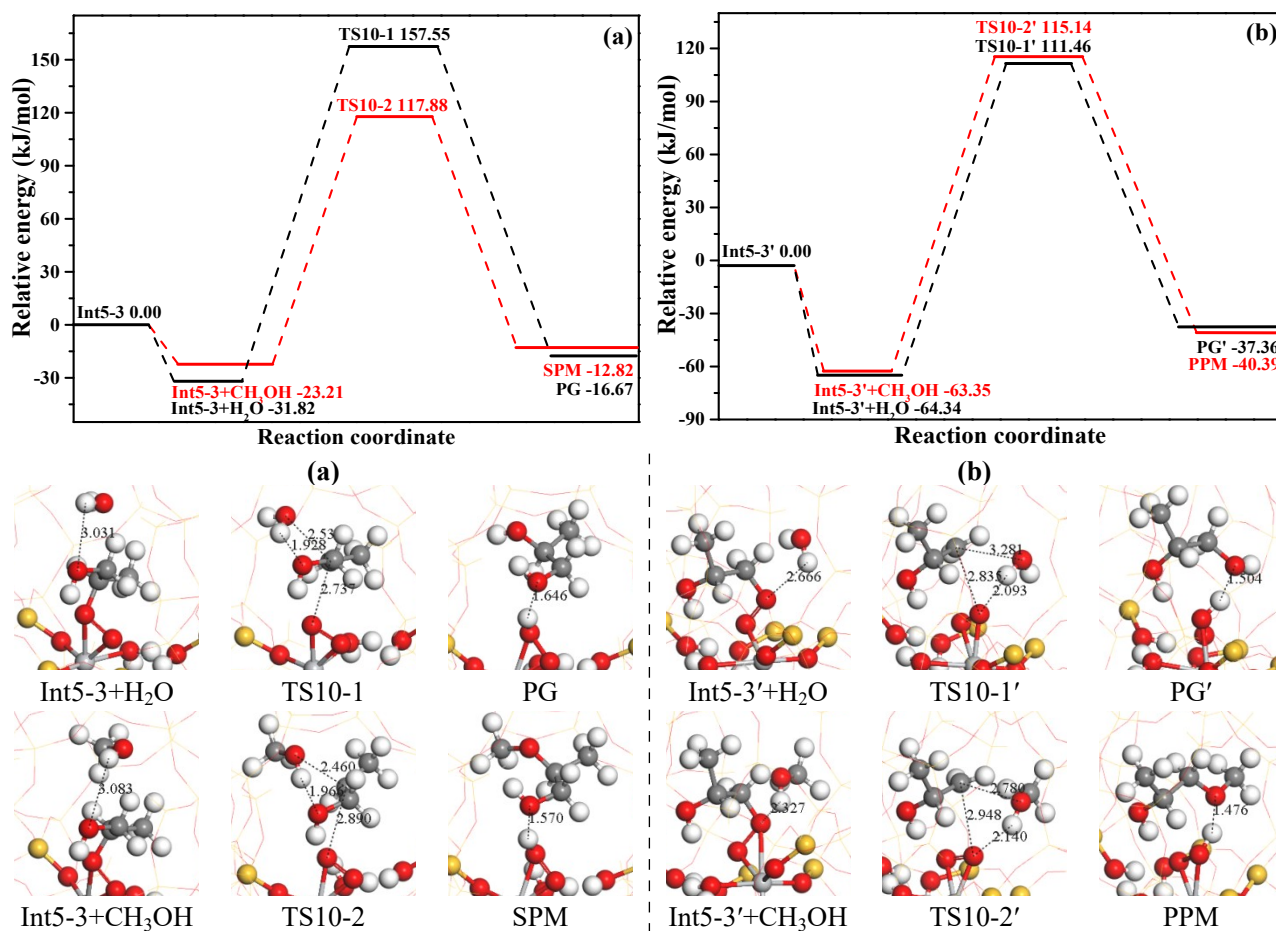


**Fig. S8** Potential energy profiles of PG and MME formation via 3MR Ti-OOH at 313 K together with together with the structures of reactant, transition state and product at Ti/defect site. The energy unit is in kJ/mol, and bond length is in Å (Ti = light grey, C = grey, O = red, Si = yellow, H = white).

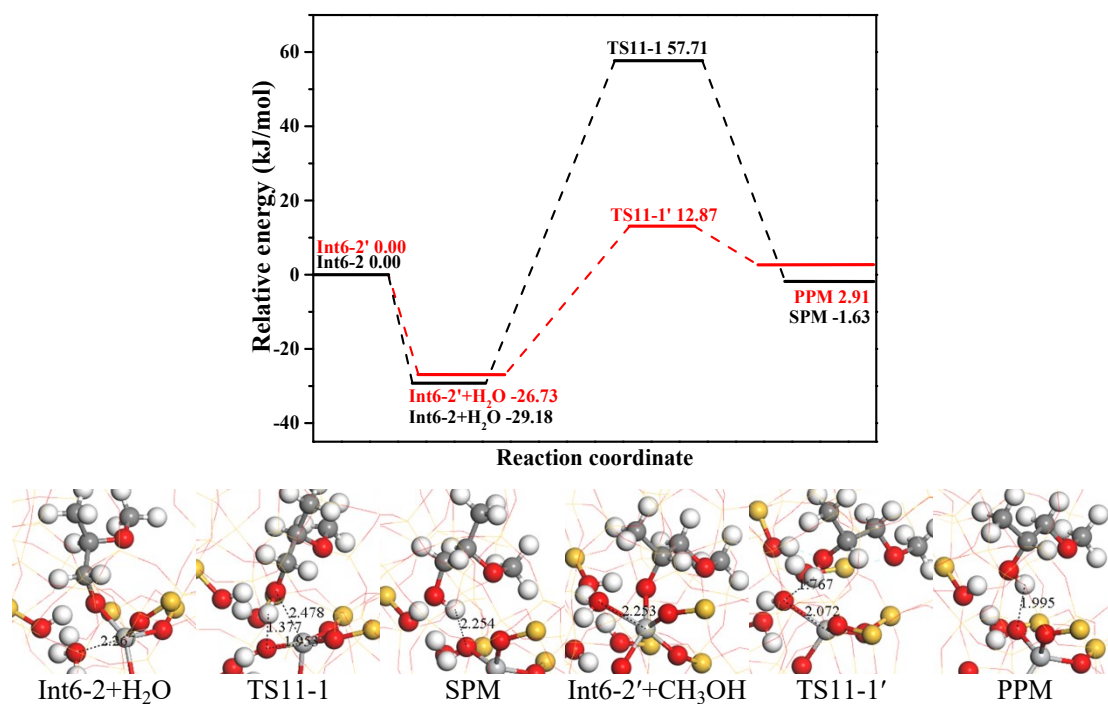


**Fig. S9** Potential energy profiles for MME formation *via* hydrolysis of Int6-2 and Int6-2' at 313 K together with the structures of reactant, transition state and product at Ti/defect site. The energy unit is in kJ/mol, and bond length is in Å. (Ti = light grey, C = grey, O = red, Si = yellow, H = white).

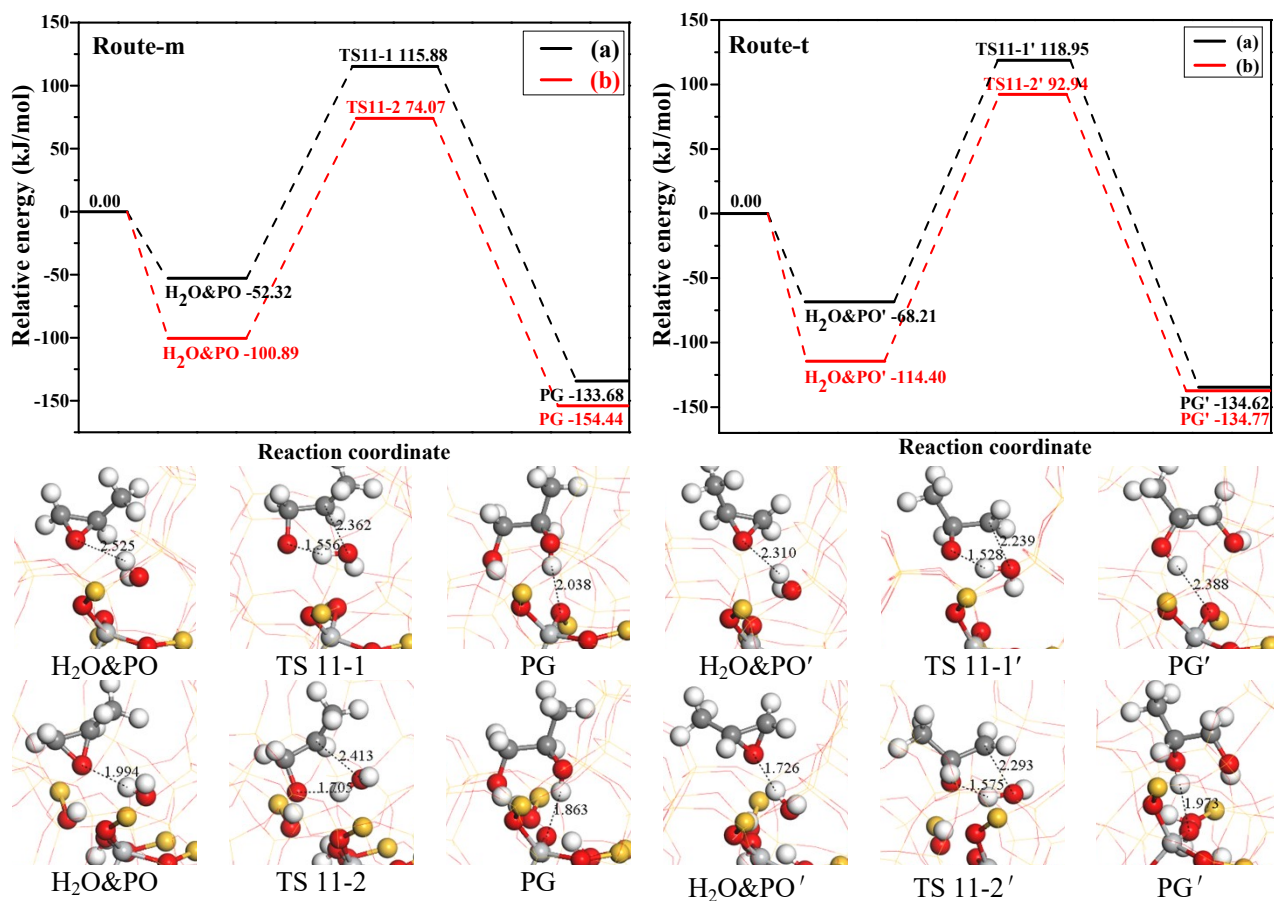


**Fig. S10** Potential energy profiles for PG formation *via* concerted mechanism at 313 K together with together with the structures of reactant, transition state and product at (a) tetrahedral Ti and (b) Ti/defect sites. The energy unit is in kJ/mol, and bond length is in Å. (Ti = light grey, C = grey, O = red, Si = yellow, H = white).

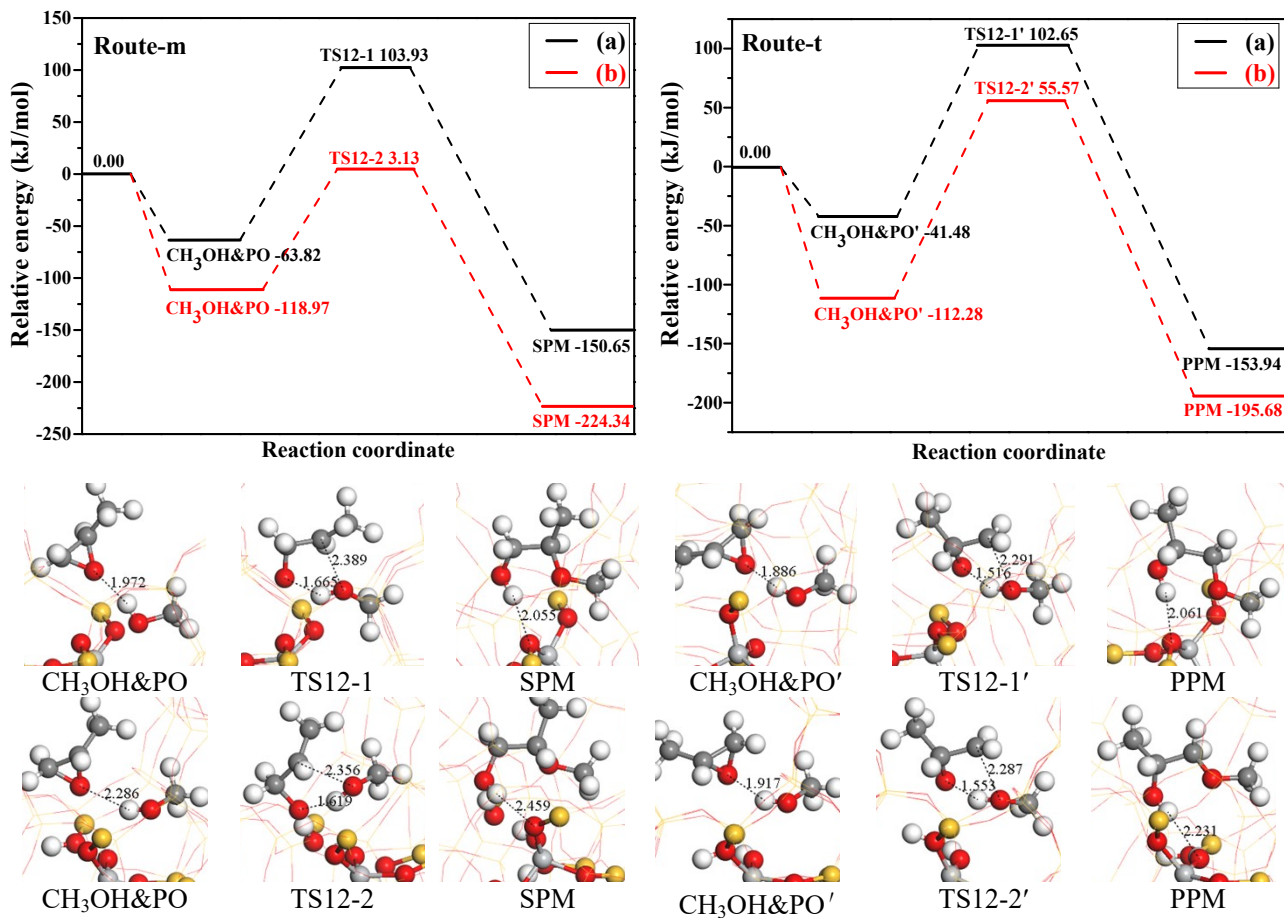


**Fig. S11** Potential energy profiles for SPM and PPM formations *via* concerted mechanism at 313 K together with the structures of reactant, transition state and product at (a) tetrahedral Ti and (b) Ti/defect sites. The energy unit is in kJ/mol, and bond length is in Å. (Ti = light grey, C = grey, O = red, Si = yellow, H = white).

**Table S1** The corresponding activation free energy ( $G_a$ , kJ/mol), reaction free energies ( $\Delta G$ , kJ/mol) and the only one imaginary frequency of transition states ( $\nu$ , cm<sup>-1</sup>) of ring-opening active substances formation at tetrahedral Ti and Ti/defect sites (T=313 K).

TS-1 models	TSs	$G_a$ , kJ/mol	$\Delta G$ , kJ/mol	$\nu$ , cm <sup>-1</sup>
Tetrahedral site	TS1-1	152.74	113.35	-316.51
	TS1-2	127.26	96.03	-1058.56
	TS1-3	121.84	87.72	-1034.42
Ti/defect site	TS2-1	29.31	-31.40	-630.65
	TS2-1	45.56	-35.34	-658.59
	TS2-3	59.04	-49.06	-793.13

**Table S2** The corresponding activation free energy ( $G_a$ , kJ/mol), reaction free energies ( $\Delta G$ , kJ/mol) and the only one imaginary frequency of transition states ( $\nu$ , cm<sup>-1</sup>) for Brønsted acid reaction mode of PO with Ti-OH at tetrahedral Ti and Ti/defect sites (T=313 K).

TS-1 models	TSs	$G_a$ , kJ/mol	$\Delta G$ , kJ/mol	$\nu$ , cm <sup>-1</sup>
Tetrahedral Ti site	TS3-1	92.43	25.35	-262.35
	TS3-1'	106.27	-35.36	-450.01
	TS3-2	102.31	-43.81	-354.92
	TS3-2'	125.66	-67.65	-452.37
Ti/defect site	TS5-1	78.88	-74.71	-444.37
	TS5-1'	136.44	-72.77	-498.61

**Table S3** The corresponding activation free energy ( $G_a$ , kJ/mol), reaction free energies ( $\Delta G$ , kJ/mol) and the only one imaginary frequency of transition states ( $\nu$ , cm<sup>-1</sup>) for Lewis acid reaction mode of PO with Ti-OH over tetrahedral Ti and Ti/defect sites (T=313 K).

TS-1 models	TSs	$G_a$ , kJ/mol	$\Delta G$ , kJ/mol	$\nu$ , cm <sup>-1</sup>
Tetrahedral site	TS4-1	167.80	-29.99	-342.06
	TS4-1'	160.68	-21.71	-508.35
Ti/defect site	TS6-1	106.51	-89.74	-234.90
	TS6-1'	124.20	-73.49	-499.54

**Table S4** The corresponding activation free energy ( $G_a$ , kJ/mol), reaction free energies ( $\Delta G$ , kJ/mol) and the only one imaginary frequency of transition states ( $\nu$ , cm<sup>-1</sup>) for Lewis acid reaction mode of PO with Ti-OCH<sub>3</sub> at tetrahedral Ti and Ti/defect sites (T=313 K).

TS-1 models	TSs	$G_a$ , kJ/mol	$\Delta G$ , kJ/mol	$\nu$ , cm <sup>-1</sup>
Tetrahedral site	TS5-1	263.18	-41.22	-303.27
	TS5-1'	289.62	-41.90	-318.17
Ti/ddefect site	TS6-2	89.41	-88.19	-286.60
	TS6-2'	132.11	-95.69	-329.57

**Table S5** The corresponding activation free energy ( $G_a$ , kJ/mol), reaction free energies ( $\Delta G$ , kJ/mol) and the only one imaginary frequency of transition states ( $\nu$ , cm<sup>-1</sup>) for PO with Ti-OOH at tetrahedral Ti and Ti/defect sites (T=313 K).

TS-1 models	TSs	$G_a$ , kJ/mol	$\Delta G$ , kJ/mol	$\nu$ , cm <sup>-1</sup>
Tetrahedral site	TS3-3	134.25	-17.50	-352.27
	TS3-3'	153.70	-24.23	-368.42
Ti/ddefect site	TS5-2	120.55	-76.51	-378.37
	TS5-2'	217.83	-40.41	-481.83
	TS5-3	52.52	-123.66	-281.55
	TS5-3'	90.80	-96.23	-326.91

**Table S6** The corresponding activation free energy ( $G_a$ , kJ/mol), reaction free energies ( $\Delta G$ , kJ/mol) and the only one imaginary frequency of transition states ( $\nu$ ,  $\text{cm}^{-1}$ ) for PG formation via stepwise mechanism at tetrahedral Ti and Ti/defect sites (T=313 K).

TS-1 models	TSs	$G_a$ , kJ/mol	$\Delta G$ , kJ/mol	$\nu$ , $\text{cm}^{-1}$
Tetrahedral site	TS7-1	21.36	-93.55	-309.33
	TS7-1'	30.46	-49.56	-325.64
	TS8-1	188.06	33.38	-332.83
	TS8-1'	128.75	-18.70	-280.02
Ti/defect site	TS9-1	50.19	28.46	-151.31
	TS9-1'	73.29	65.45	-218.87
	TS9-2	72.24	43.86	-253.81
	TS9-2'	42.18	8.47	-214.09
	TS10-1	189.37	15.15	-269.82
	TS10-1'	175.80	26.98	-234.44

**Table S7** The corresponding activation free energy ( $G_a$ , kJ/mol), reaction free energies ( $\Delta G$ , kJ/mol) and the only one imaginary frequency of transition states ( $\nu$ ,  $\text{cm}^{-1}$ ) for MME formation via stepwise mechanism at tetrahedral Ti and Ti/defect sites (T=313 K).

TS-1 models	TSs	$G_a$ , kJ/mol	$\Delta G$ , kJ/mol	$\nu$ , $\text{cm}^{-1}$
Tetrahedral site	TS7-2	11.67	-99.10	-281.14
	TS7-2'	34.93	-32.95	-345.37
	TS8-2	185.55	10.04	-364.02
	TS8-2'	137.86	-31.89	-345.37
Ti/defect site	TS9-3	188.24	-8.99	-337.34
	TS9-3'	146.29	-17.15	-290.49
	TS10-2	141.09	10.39	-294.66
	TS10-2'	178.49	22.96	-327.77
	TS11-1	86.89	27.56	-302.84
	TS11-1'	39.60	29.64	-300.94



**Table S8** The corresponding activation free energy ( $G_a$ , kJ/mol), reaction free energies ( $\Delta G$ , kJ/mol) and the only one imaginary frequency of transition states ( $\nu$ , cm<sup>-1</sup>) of MME formation *via* concerted mechanism at tetrahedral Ti and Ti/defect sites (T=313 K).

TS-1 models	TSs	$G_a$ , kJ/mol	$\Delta G$ , kJ/mol	$\nu$ , cm <sup>-1</sup>
Tetrahedral site	TS11-1	168.20	-81.36	-464.38
	TS11-1'	187.16	-66.41	-556.30
Ti/ddefect site	TS11-2	174.96	-53.55	-412.72
	TS11-2'	207.34	-83.40	-448.98

**Table S9** The corresponding activation free energy ( $G_a$ , kJ/mol), reaction free energies ( $\Delta G$ , kJ/mol) and the only one imaginary frequency of transition states ( $\nu$ , cm<sup>-1</sup>) of MME formation *via* concerted mechanism at tetrahedral Ti and Ti/defect sites (T=313 K).

TS-1 models	TSs	$G_a$ , kJ/mol	$\Delta G$ , kJ/mol	$\nu$ , cm <sup>-1</sup>
Tetrahedral site	TS12-1	167.75	-86.83	-544.34
	TS12-1'	144.13	-112.46	-517.88
Ti/ddefect site	TS12-2	122.10	-105.37	-562.16
	TS12-1'	167.85	-83.40	-534.01